Macromolecules **2002,** *35,* 6483−6485

Aggregation and Surface Morphology of a Poly(ethylene oxide)-*block*-polystyrene Three-Arm Star Polymer at the Air/Water Interface Studied by AFM

Raju Francis,[†,‡,§] **Andrew M. Skolnik,**[†]
Stephen R. Carino,[†] **Jennifer L. Logan,**[†,‡]
Royale S. Underhill,[†] **Stéphanie Angot,**[‡]
Daniel Taton,[‡] **Yves Gnanou,**[‡] **and**
Randolph S. Duran*[,†]

The George and Josephine Butler Polymer Research Laboratory, Department of Chemistry, University of Florida, P.O. Box 117200, Gainesville, 32611-7200; and Laboratoire de Chimie des Polymères Organiques, ENSCPB, University of Bordeaux I, 16 Avenue Pey−Berland, 33607 Pessac Cedex, France

Received February 21, 2002

1. Introduction. Amphiphilic diblock copolymers are widely used as agents to alter the interfacial properties of paints, personal care products, detergents, printing agents and pharmaceutical preparations. The monolayer behavior at the air/water interface of these copolymers, particularly poly(ethylene oxide)-*block*-polystyrene (PEO-*b*-PS) based systems has been of interest during the past few years.[1−10] The formation of surface micelles or aggregation at the air/water interface has been observed for linear PEO-*b*-PS systems, but there are no reports on PEO-*b*-PS-based stars under similar conditions.

Star−block copolymers present a promising system for studying highly branched polymeric architectures. Recent advances in the area of controlled radical polymerization[11] by nitroxide-mediated polymerization (NMP),[12,13] atom transfer radical polymerization (ATRP),[14,15] and reversible addition−fragmentation transfer (RAFT)[16] have contributed to the synthesis of novel macromolecular architectures such as stars, dendrimers, and hyperbranched polymers.

There are three mechanisms proposed in the literature which describe domain formation at the air/water interface. All three mechanisms assume a linear block copolymer with hydrophilic and hydrophobic blocks. Goncalves da Silva et al. postulated that block copolymers form micelles in solution prior to spreading and upon deposition form surface micelles which become more densely packed with increased surface pressure.[17] An et al. and Isrealachvili both suggested that the polymers are deposited as unimers onto the subphase and only aggregate upon compression.[18,19] Recently Cox et al. have established that linear block copolymers deposit as a combination of the first two models. Unimers deposit and spontaneously surface aggregate.[9] The aggregates become denser upon compression.

In this work, we investigate the behavior of a three-arm star amphiphilic copolymer, PEO_3-*b*-PS_3, at the air/water interface through AFM images of the monolayer on mica.

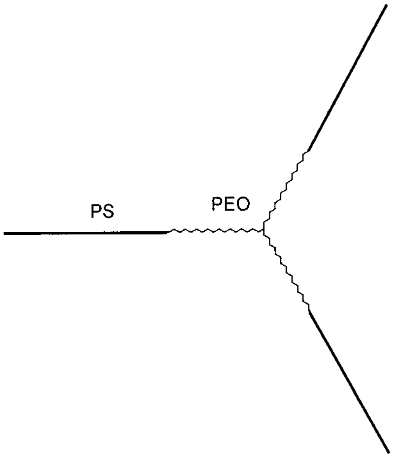

Figure 1. Conformation of star copolymer. 45 repeat units PEO/arm; 77 repeat units PS/arm; $M_n = 30\,000$; PDI = 1.3.

The results reported assume that the characteristics of the monolayer at the air/water interface remain unchanged upon transfer to the mica surface.

2. Experimental Section. The PEO_3-*b*-PS_3 three-arm star used in this study was prepared first by the anionic polymerization of ethylene oxide followed by the ATRP synthesis of styrene and has been reported previously.[20] This three-arm star polymer has a number-average molecular weight (M_n) of 30 000 with a polydispersity index of 1.3 as determined elsewhere.[20] The poly(ethylene oxide) and polystyrene blocks per arm correspond to 45 ethylene oxide and 77 styrene units respectively, leading to an average molecular weight of 10 000 for each arm (Figure 1).

Spectroscopic grade chloroform (Sigma-Aldrich) was used as the spreading solvent without further purification. A fresh piece of mica substrate (length × width ∼ 50×16 mm^2 and thickness = 0.1 mm) was cleaved prior to use.

The Langmuir−Blodgett (LB) films were prepared on a KSV 5000 system (KSV Instruments Ltd.) with a platinum Wilhelmy plate. The subphase was 18 MΩ cm^{-1}, ultrafiltered water (Milli-Q Millipore system equipped with an organic removal cartridge). The temperature of the subphase was maintained at 25 ± 0.5 °C. For all experiments, the subphase was prepared, followed by the immersion of the substrate and Wilhelmy plate. Then, 50 μL of the polymer solution (∼1 mg mL^{-1} in $CHCl_3$) was spread evenly over the water surface in small (approximately 2 μL) drops. The solvent was allowed to evaporate for 30 min. The polymer film was compressed until the desired transfer surface pressure was reached. To deposit the monolayer, the substrate was slowly (1 mm min^{-1}) withdrawn vertically through the interface, while a constant surface pressure was maintained. On the basis of the recorded isotherm, the corresponding mean molecular area (MMA) (the average area one molecule occupies at the air/water interface) was obtained. After transfer, the mica plate was dried at room temperature for 24 h.

Atomic force microscopy was performed using a “J” scanner on a NanoScope III system (Digital Instruments) in tapping mode with sharp silicon cantilevers ($T = 3.8{-}4.5$ μm, $W = 27.6{-}29.2$ μm and $L = 131$ μm, Nanosensors). Acquired images were flattened using a

---

* To whom all correspondence should be addressed. Telephone: 352-392-2011. Fax: 352-392-9741. E-mail: duran@chem.ufl.edu.

[†] University of Florida.

[‡] University of Bordeaux I.

[§] Permanent address: Department of Chemistry, St. Joseph’s College, University of Calicut, Kerala-673 008, India.

10.1021/ma020290z CCC: $22.00

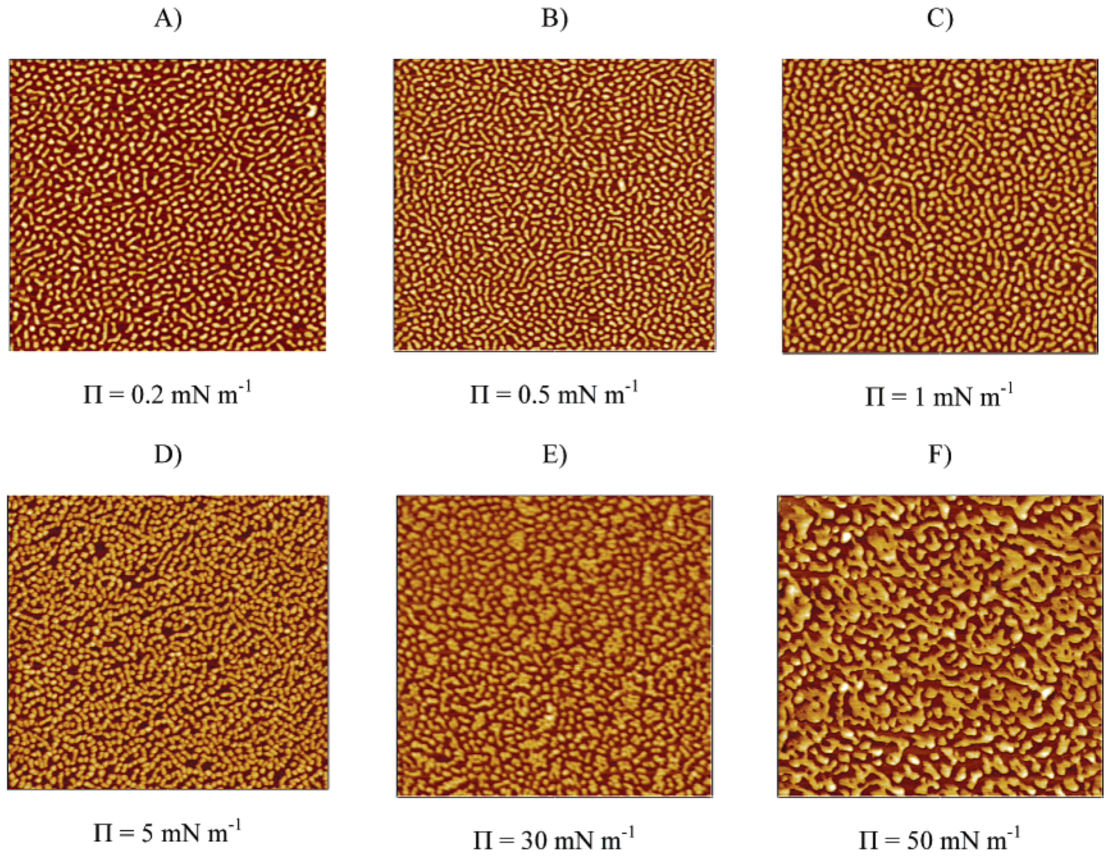

Figure 2. AFM images of PEO_3-*b*-PS_3 star polymer monolayer on a mica surface. The horizontal scale is 2 μm, and the vertical scale is 10 nm. The bright domains are PS, and the dark domains are PEO.

Table 1. Characteristics of LB Film Experiment[a]

run	surface pressure (mN/m)	mean molecular area (MMA) (Å^2)	transfer ratio
A	0.2	5950	1.097
B	0.5	5330	1.844
C	1	4950	1.086
D	5	3360	1.124
E	30	2070	0.657
F	50	1750	0.735

[a] Temperature = 25 ± 0.5 °C.

Table 2. AFM Characteristics of PEO_3-*b*-PS_3 Three-Arm Star Polymer

surface pressure (mN/m) (±0.05)	av diam of PS domains (nm) (±7)	vertical dist (nm) (±1)	no. of domains (±50)	PS coverage area[a] (%) (±10)	no. of molecules per domain (±10)
0.2	27	3	1229	18	55
0.5	31	3	1353	25	47
1	35	4	1401	34	58
5	42	4	1735	78	69
30	58	4	1684	N/A[b]	115

[a] Total area = 4 × 10^8 Å^2. [b] At a surface pressure of 30 mN/m, film is in a multilayer regime.

second order flattening routine in the Digital Instruments software. Domain sizes were measured using a section analysis tool in the same software.

3. Results and Discussion. The experimental variables are summarized in Table 1. Surface pressures chosen for film preparation were determined based on the slope variations of a $\Pi - A$ isotherm obtained previously.[18] The variations in the slope of the isotherm indicated a change in how the polymer was organizing in the subphase. In each case, a positive transfer ratio was observed indicating transfer of film onto the mica surface. The LB film deposition on mica was prepared separately at various pressures since a layer effect was observed when different parts of the same piece of mica were used at different pressures.

Once dry, a small portion of the mica was cut for AFM imaging. The piece was taken from the center of the sample to avoid hysteresis effects. Fresh cantilevers (AFM tips) for each sample were used since image degradation was observed when the same tip was used for imaging subsequent samples. Parts A−F of Figure 2 show the AFM images recorded at different surface pressures. In all cases, the horizontal scale was set to 2 μm and the vertical scale was set to 10 nm. Parts A−F of Figure 2 correspond to runs A−F presented in Table 1.

At surface pressures <5 mN/m, a hexagonally packed pattern of higher elevation PS spheres, sometimes chained to form rods, surrounded by lower elevation PEO regions was observed. As seen in Figure 2, an evolution of structure from sphere-rich to rod-rich domains (A−D) and then to aggregate and multilayer structures (E, F) is observed with increased compression. In the AFM images, it was assumed that there was no vacant space between the domains. This assumption yielded a better approximation in calculating the domain area (Table 2).

PEO will spread at the surface due to an attraction to the water. Both the PEO and the water surface, however, repel the hydrophobic PS. The repulsion leads to aggregation. Thus, the higher elevation domains observed in the AFM images are PS while the continuous phase surrounding them is PEO. The horizontal and vertical distances presented in Table 2 correspond to the average diameter and height of the spherical (polystyrene) domains. The total number of domains was determined by manual count (experimental error is indicated in brackets). The PS coverage area was calculated by taking the area of the polystyrene domain multiplied by the total number of polystyrene domains and divided by the total area of the image ($2 \times 2\ \mu m^2$). The number of PEO3-*b*-PS_3 star molecules per domain was calculated by dividing the total area by the number of domains and then dividing by the MMA at the different transfer pressures. The large number of molecules per domain, ~50, is not easily explained by any simple geometric model we know of, though PS chains are presumably highly intertwined. The data shows that on changing the surface pressure from $\Pi = 0.2$ mN m^{-1} to $\Pi = 50$ mN m^{-1} the packing of domains (or aggregates) becomes closer, ultimately resulting in collapse of the monolayer (Figure 2F). These results, for star copolymers, agree with the idea proposed by Lennox and co-workers for linear block copolymers: that surface aggregation is a spontaneous process, which is neither compression nor spreading solvent dependent.[9] Similar to observations made by Lennox, these results show spontaneous aggregate formation after spreading as evidenced by AFM at very low pressure (Figure 2A). Alternately, a surface pressure dependent change in domain size and conformation can be seen in moving from Figure 2A to Figure 2F (see also Table 2). The PS coverage area shows a large increase in size with increasing surface pressure consistent with the hypothesis that aggregates become denser on compression. The number of molecules per domain is similar at low pressures and may increase at higher pressures. This may be due to the sphere to rod transformation of the monolayer.

A sphere to rod transition is consistent with the morphology model proposed by Floudas et al. [21] For this PEO_3-*b*-PS_3 star, the fraction of PS is $f_{ps} = 0.53$. Using the phase diagram predicted for a four-arm star in bulk as χN increases, the morphology changes from spheres to rods to gyroid.[21]

In the work presented here, we hypothesize that the increase in Π corresponds to an increase in χ, and we observe the predicted change in morphology, even in a 2D monolayer.

4. Conclusion. These results report for the first time the behavior of a PEO_3-*b*-PS_3 three-arm star polymer at the air/water interface. Spontaneous aggregation was observed after spreading the polymer solution on the surface of water. These aggregates move closer together and increase in size with increasing surface pressure. Well-defined, hexagonally packed spherical domains were seen at low pressures. This morphology was followed by rod-rich morphologies at intermediate pressures. At higher pressures, clusters and collapse of the film occur.

Acknowledgment. Support from DOE-BES and NSF/CNRS Grant No. DE-FG02-01ER45933 and NSF Grant No. INT-9816175 is acknowledged. J.L.L. acknowledges support from the NSF Graduate Fellowship Program.

References and Notes

(1) Shuler, R. L.; Zisman, W. A. *J. Phys. Chem.* **1970**, *74*, 1523.
(2) Harris, J. M. *Poly(ethylene glycol) Chemistry-Biotechnical and Biomedical Applications*; Plenum Press: New York, 1992.
(3) Yu, K.; Eisenberg, A. *Macromolecules* **1998**, *31*, 3808.
(4) Mortensen, K.; Brown, W.; Almdal, K.; Alami, E.; Jada, A. *Langmuir* **1997**, *13*, 3635.
(5) Xu, R.; Winnik, M. A.; Reiss, G.; Chu, B.; Croucher, M. D. *Macromolecules* **1992**, *25*, 644.
(6) Guzonas, D.; Boils Hair, M. L. *Macromolecules* **1991**, *24*, 3883.
(7) Pagac, E. S.; Prieve, D. C.; Solementsev, Y.; Tilton, R. D. *Langmuir* **1997**, *13*, 2993.
(8) Baker, S. M.; Callahan, A.; Smith, G.; Toprakcioglu, C.; Vradis, A. *Physica B* **1998**, *241*, 1041.
(9) Cox, J. K.; Constantino, B.; Yu, K.; Eisenberg, A.; Lennox, R. B. *Langmuir* **1999**, *15*, 7714.
(10) Cox, J. K.; Yu, K.; Eisenberg, A.; Lennox, R. B. *Phys. Chem. Chem. Phys.* **1999**, *1*, 4417.
(11) Matyjaszewski, K. *Controlled/Living radical Polymerization: Progress in ATRP, NMP and RAFT*; ACS Symposium Series 768; American Chemical Society: Washington, DC, 2000.
(12) Benoit, D.; Grimaldi, S.; Robin, S.; Finet, J.-P.; Tordo, P.; Gnanou, Y. *J. Am. Chem. Soc.* **2000**, *122*, 5929.
(13) Hawker, C. J.; Bosman, A. W.; Harth, E. *Chem. Rev.* **2001**, *101*, 3661.
(14) Matyjaszewki, K.; Xiz, J. *Chem. Rev.* **2001**, *101*, 2921.
(15) Kamigaito, M.; Ando, T.; Sawamoto, M. *Chem. Rev.* **2001**, *101*, 3689.
(16) Rizzardo, E.; Chiefari, J.; Chong, Y. K.; Ercole, F.; Krstina, J.; Jeffrey, J.; Le, T. P.; Mayadunne, R. T.; Meijs, G. F.; Moad, G.; Moad, C. L. *Macromol. Symp.* **1999**, *143*, 291.
(17) Goncalves da Silva, A. M.; Simoes Gamboa, A. L.; Martinho, J. M. G.; *Langmuir* **1998**, *14*, 5327.
(18) An, S. W.; Su, T. J.; Thomas, R. K.; Baines, F. L.; Billingham, N. C.; Armes, S. P.; Penfold, J. *J. Phys. Chem. B* **1998**, *102*, 387.
(19) Israelachvili, J. *Langmuir* **1994**, *10*, 3774.
(20) Angot, S.; Taton, D.; Gnanou, Y. *Macromolecules* **2000**, *33*, 5418.
(21) Floudas, G.; Pispas, S.; Hadjichristidis, N.; Pakula, T.; Erukhimovich, I. *Macromolecules* **1996**, *29*, 4142.

MA020290Z